Scientific Research Publishing

Open Journal of Air Pollution, 2023, 12, 1-29
https://www.scirp.org/journal/ojap
ISSN Online: 2169-2661
ISSN Print: 2169-2653

June to October Aerosol Optical Depth over the Arctic at Various Spatial and Temporal Scales in MODIS, MAIAC, CALIOP and GOES Data

Nicole Mölders[1,2], Mariel Friberg[3,4]

[1]Department of Atmospheric Sciences, College of Natural Science and Mathematics, University of Alaska Fairbanks, Fairbanks, USA
[2]Geophysical Institute, University of Alaska Fairbanks, Fairbanks, USA
[3]National Aeronautics and Space Administration, Goddard Space Flight Center, Greenbelt, USA
[4]Earth System Science Interdisciplinary Center, University of Maryland, College Park, USA

Email: cmoelders@alaska.edu

How to cite this paper: Mölders, N. and Friberg, M. (2023) June to October Aerosol Optical Depth over the Arctic at Various Spatial and Temporal Scales in MODIS, MAIAC, CALIOP and GOES Data. *Open Journal of Air Pollution*, **12**, 1-29.
https://doi.org/10.4236/ojap.2023.121001

Received: November 30, 2022
Accepted: February 25, 2023
Published: February 28, 2023

Abstract

The accuracy of the cloud-aerosol lidar with orthogonal polarization (CALIOP), moderate resolution imaging spectroradiometer (MODIS), Multi-Angle Implementation of Atmospheric Correction (MAIAC), and Geostationary Operational Environmental Satellite (GOES) aerosol optical depth (AOD) products for the Arctic north of 59.75˚N was examined by means of 35 aerosol robotic network (AERONET) AOD sites. The assessment for June to October 2006 to 2020 showed MAIAC AOD agreed the best with AERONET AOD; CALIOP AOD differed the strongest from the AERONET AOD. Cross-correlations of CALIOP AOD along the satellite path indicated that AOD-values 40 km up-and-down the path often failed to represent the AERONET AOD-values within ±30 min of the overpass in this region dominated by easterly winds. Typically, CALIOP AOD was lower than AERONET AOD and MAIAC AOD at the sites, especially, at sites with mean AOD below 0.1. Generally, MODIS AOD values exceeded those of MAIAC. Comparison of CALIOP, MAIAC, and MODIS products resampled on a 0.25˚ × 0.25˚ grid revealed differences among the products caused by their temporal and spatial resolution, sample habit and size. Typically, the MODIS AOD-product showed the most details in AOD distribution. Despite differences in AOD-values, all products provided similar temporal evolution of elevated and lower AOD.

Keywords

Inter-Comparison of MAIAC CALIOP MODIS C6.1 GOES AOD-Products, Long-Term Evaluation of AOD-Products with AERONET Observations,

AOD Distribution over the Arctic, Changes in Arctic AOD Climatology

1. Introduction

Both passive and active remote-sensing techniques on board Polar-Earth orbiting satellites permit studying the atmosphere in regions of scarce surface observations like the oceans and Arctic. Retrieval algorithms interpret the observations in terms of aerosol optical depth (AOD), among other things (cf. [1] [2] [3]). Passive radiometric AOD retrievals rely mainly on scattered radiances limiting their application to daytime and cloud-free conditions. Examples are the moderate resolution imaging spectroradiometer (MODIS) and Multi-Angle Implementation of Atmospheric Correction (MAIAC) aerosol products.

The Cloud-Aerosol Lidar with Orthogonal Polarization (CALIOP), onboard the National Aeronautics and Space Administration (NASA) and Centre National d' Études Spatiales (CNES) Cloud-Aerosol Lidar and Infrared Pathfinder Satellite Observation (CALIPSO), can observe AOD also during darkness [4]-[9].

Scientists use predictions from chemistry transport, climate, and Earth system models (e.g. [10]) for solar energy [11] and air quality assessments [12]. They rely on spatially distributed AOD data like the CALIOP, MAIAC, and MODIS data for simulated AOD evaluation and improvements. However, satellite-borne instrument data accuracy must be assessed using ground-based observations. For this purpose, the aerosol robotic network (AERONET), AERONET Maritime Aerosol Network (MAN), and other networks with standardized instrument calibration protocols have been established to improve space-borne retrievals.

Several studies compared sun-photometer to satellite-retrieved AOD and inter-compared various AOD satellite retrieval algorithms. Their major findings were as follows. According to the comparison of MODIS Aqua and Terra Level (L) 3 daily mean AOD at 470, 550, and 660 nm with daily mean AERONET L2 data from 452 sites with at least one year of observations during the 2000-2018 timeframe, Aqua AOD data performed better than those of Terra. Furthermore, the MODIS AOD accuracy differed with the Köppen-Geiger climate for all three wavelengths [11]. The combined Aqua and Terra AOD absolute root-mean-square error (RMSE) and mean absolute error were 0.106 and 0.109, respectively.

A study by [5] reported an over-ocean AOD expected error (EE) for 3 km MODIS Aqua (MYD_3k) of $\pm(0.04 + 0.05\tau)$, where τ is the 550 nm AERONET/MAN value. In the case of 10 km MODIS Collection (C) 6 AOD, 76.16% of the over-ocean data fall within the reported EE limits with a correlation coefficient of 0.937 [5]. For MODIS C6.1 AOD, the over-land and over-ocean EE are $\pm(0.05 + 0.15\tau)$ and $\pm(0.05 + 0.03\tau)$, respectively [13].

Comparison of 3 km MODIS C6.1 550 nm AOD with 20 coastal AERONET

and MAN sites north of 59.9˚N for the June to October shipping season from 2006 through 2018 revealed the following [12]. Typically, MODIS C6.1 AOD exceeded that of AERONET at low values, whereas the opposite was true at high values. The MODIS C6.1 and AERONET AOD differed strongest for sites in very heterogeneous environments, such as the Canadian Archipelago and coast of Greenland. The MODIS C6.1 and MAN AOD differed stronger west of Greenland and over the Bering Sea than in the Greenland and Norwegian Seas and Atlantic. The inter-seasonal MODIS C6.1 and AERONET AOD variability was strongly correlated (R = 0.933). Due to errors in sea ice vs. open water classification, agreement between MODIS C6.1 and MAN AOD improved with time during the shipping season. Overall, 75.3% and 87.5% to 100% of the combined Terra and Aqua MODIS C6.1 AOD were within the limits of the EE over land and ocean, respectively [12].

Currently, MAIAC is considered to have the highest accuracy [5]. Over South Asia and South America, the MAIAC EE was determined as $\pm(0.05 + 0.05\tau)$ [14]. When compared with collocated AERONET AOD, MAIAC and MODIS dark target (DT) and blue target (BT) AOD data had comparable statistical performance over relatively dark surfaces over eastern North America. Over the inhomogeneous elevations and bright surfaces of western North America, however, MAIAC AOD outperformed the DT and BT retrievals [15]. The systematic positive bias of DT retrievals occurred over bright surfaces, whereas BT and MAIAC retrievals showed no such bias. Additionally, MAIAC had the lowest spread in error [15].

The narrow CALIOP swath width limits the opportunities to assess AOD. Clouds permitting, the minimum coincidence time between CALIOP and sun-photometer measurements can be as large as 16 days at the Equator. Although overpasses may occur more often over the Arctic Ocean between 70˚N and 80˚N, the Arctic Ocean cloud coverage is significantly higher (70% ± 30% during the boreal summer [16]) than at low latitudes.

According to Omar and Holben [pers. Comm.], the CALIOP EE is $\pm(0.05 + 0.4\tau)$. The three-year comparison between CALIOP L2 and sun-photometer data over Wuhan and Dengfeng (China) yielded absolute biases of 0.22 ± 0.21, 0.11 ± 0.07, and 0.14 ± 0.13 under clean, moderate, and polluted conditions, respectively. CALIOP fails to detect weak aerosol layers leading to an AOD underestimation of 0.05 or less [17]. Consequently, there may be potential bias of CALIOP AOD over clean Arctic Ocean regions when background AOD is less than 0.05.

Collocated global- and zonal-means of CALIOP and MODIS AOD differ stronger over ocean than land; however, CALIOP AOD values were roughly within the range of the MODIS expected uncertainty [17]. Over the Yellow River region from 2007 to 2014, the MODIS C6.1 AOD agreed best in winter, followed by fall, summer, and spring. For AOD less than 0.3, differences were minor; above this threshold, differences increased with increasing MODIS AOD [18]. As expected, the CALIOP and MODIS AOD agreement is sensitive to the prod-

uct spatial resolution. For instance, CALIOP AOD agreed better with the 10 km MODIS product than the 3 km product.

An inter-comparison of 14 satellite-retrieved AOD-products [19] revealed that product biases varied differently among regions. Typically, satellite- and AERONET-retrieved AOD correlated stronger over land than ocean. On average, 1˚ × 1˚ resolution AOD under- and overestimates were between 15% and 25%, with outliers reaching up to ±50%. The authors attributed approximately 50% of the discrepancies to cloud contamination. They also showed how AOD uncertainty maps were used to assess performance as a function of distance from AERONET sites.

Previous inter-comparison studies focused on mid and low latitudes, whereas the goal of our study was to compare CALIOP, MODIS, and MAIAC aerosol products over the Arctic. To achieve this objective, we 1) assessed CALIOP, MODIS C6.1 and MAIAC AOD retrievals by means of sun-photometer data, and 2) examined the role of spatial scales of collocation for obtained accuracy over the Arctic north of 59.75˚N for June to October 2006 to 2020. The high temporal resolution Geostationary Operational Environmental Satellite (GOES-R) series AOD-product was included only for the 2020 temporal analysis, when the two platforms (GOES-16/17) were operational.

2. Descriptions of the Aerosol Optical Depth Data, Experimental Design, and Analysis Methodology

This section describes briefly the CALIOP, MODIS and MAIAC aerosol optical depth products, and the sun-photometer aerosol optical depth data used for their assessment, the data processing applied for this assessment and the inter-comparison of AOD products, as well as the analysis methods applied to examine the role of spatial scales of collocation.

Typically, satellite-retrieved and ground-based data are assumed to collocate for overpasses within ±30 min in a 40 km radius of the site. Due to the different temporal and spatial scales of the ground and satellite observations, the comparison relies on the fact that turbulence influences an air mass much less than the flow does [20]. The spatial mean AOD values within the 40 km radius can be compared to the temporal mean AOD values observed within ±30 min of the overpass [21]. We assumed collocation for satellite- and surface-based observations using this procedure.

2.1. Satellite-Retrieved Aerosol Optical Depth Products and Ground-Based Aerosol Optical Depth Observations

Terra, Aqua, and CALIPSO are in Sun-synchronous polar orbits crossing the Equator at 10:30, 13:30, and 13:32 local time. The orbits repeat approximately every 16 days. The 98.2˚ retrograde orbit restricts the poleward extent of the ground track to about 80˚N.

CALIOP and MODIS are on board CALIPSO and Aqua, respectively, in the A-Train constellation. These satellites are in the same orbit with a time gap of

less than 2 minutes. Consequently, these instruments observe aerosol optical properties nearly simultaneously, allowing direct temporal comparison along the CALIOP track.

In this study, we use June through October (JJASO) data from 2006 through 2020. At nadir, the spatial resolution of the combined Aqua and Terra MODIS and CALIOP AOD-products are 3 km × 3 km and 5 km × 5 km, respectively. The MAIAC and GOES AOD-products are on a fixed 1 km and 2 km grid, respectively. The AERONET aerosol observations are point measurements.

2.1.1. MODIS Collection 6.1 Level 2 Aerosol Optical Depth Data

MODIS has 36 channels, ranging from 400 to 14,400 nm. We used the MODIS C6.1 level (L) 2 550-nm aerosol products (M[O/Y]D04 for Terra and Aqua) at 3 km increment [13]. MODIS C6.1 AOD-values at 550 nm are based on the Dark Target (DT) and Blue Target (BT) aerosol algorithms [22] [23]. A known issue with respect to collocation is that the wide variety of pixel sizes can be unbalanced in the sampling around the ground site, even at 3 km [24]. In the following, we refer to the MODIS C6.1 AOD-product as MODIS for easy readability.

2.1.2. MAIAC Version 6 Aerosol Optical Depth Data

The MAIAC Version (V) 6 aerosol products [3] are based on separate retrieval algorithms over land and ocean using data from the eight MODIS channels between 470 and 2113 nm. MAIAC assumes that surface reflectance changes related to cloud extent and aerosols change rapidly on the spatial scale. Conversely, on the temporal scale, MAIAC assumes aerosols vary slowly, permitting the assumption of constant surface reflectance holds over a limited time. The algorithm uses a background aerosol model, which was regionally tuned with AERONET optical thickness measurements [25]. The MAIAC algorithm yields AOD at 550 nm. It is calculated from the green band at 500 nm using ratios representative of the spectral slope of a given AOD. These ratios are taken from lookup tables that stem from the regionally tuned aerosol background model [3]. Over snow, MAIAC assumes an AOD of 0.05 and 0.02 at elevations over 4.2 km. Over water, MAIAC reports AOD only for glint angles ≥ 40˚ except when MAIAC detects dust with AOD-retrieved values above zero.

Known issues of the MAIAC retrieval are difficulty in accurately capturing high aerosol loading of coarse or mixed particle sizes (absolute errors between 0.5 and 1.75). Successful MAIAC retrievals marginally depend on the relative azimuth angle with generally low biases, except between 80˚ - 110˚, where matchups are very scarce. MAIAC biases are within 0.02 of the zero line for small scattering angle, but the negative bias increases once scattering angles exceed 140˚ [25].

2.1.3. CALIOP Version 4.10 Level 2 Aerosol Data

Aboard CALIPSO is a dual-wavelength and dual-polarization elastic backscatter

neodymium-doped yttrium aluminum garnet lidar, also known as CALIOP [26]. It transmits linearly polarized pulses at 532 nm and 1064 nm. The 532 nm and 1064 nm total backscatter signals and the parallel and perpendicular polarization components of the 532 nm backscatter signals permit continuous observations of aerosols and clouds [27]. For details of the data processing and retrieval algorithms, see [1]. The significantly higher lidar ratio of smoke than that of marine aerosol permits the detection of lower-level aerosol extinction for marine aerosol.

We used CALIOP V4.10 L2 retrieved aerosol data as they permit all aerosol types over the Arctic [28]. In the CALIOP dataset, a value of 0 indicates that the mass loading was below the instrument detection limits. More information on CALIOP data quality summaries, accuracy, and uncertainty can be found in [29].

2.1.4. GOES 16 and 17 Aerosol Optical Depth Data

The GOES-R Series Advanced Baseline Imager [30] [31] enables AOD retrievals using a multiband algorithm, similar to MODIS AOD retrievals. From a geostationary orbit, the 16-channel GOES-R imager generally covers the full disk of Earth once every 10 min, a region covering the Continental and Pacific US every 5 min, and mesoscale frames every 1 min. The GOES-16 and -17 platforms became operational in December 2017 and February 2019.

The GOES AOD-product exists for clear-sky pixels at view and solar zenith angles less than 90˚ during daytime [32]. Under clear-sky conditions, the current retrieval algorithm determines AOD at 550 nm every 15 min over dark surfaces. Consequently, no AOD data exist over non- or sparsely vegetated land, glaciers, snow, sea ice, and over water in the sun-glint region. Data quality tends to be less at solar zenith angles greater than 80˚ and/or satellite zenith angles greater than 60˚. Over land, biases and standard deviations of AOD below 0.04 are less than 0.06 and 0.13, respectively; For AOD between 0.04 to 0.8 (both included), biases and standard deviations remain below 0.04 and 0.25. Over water, biases and standard deviations are less than 0.15. Errors depend on the quality of calibration and navigation data, cloud and snow masks, and total precipitable water [33]. For more information, see [32] [34].

2.1.5. AERONET Version 2 Level 2 Ground-Based Aerosol Observations

The NASA AERONET [35] is equipped with CIMEL (CE-318) sun-photometers with automatic sun-sky scanning spectral radiometers. The same standard calibration procedure and AERONET V2 direct sun algorithm are used at all sites for columnar aerosol optical depth and Ångström parameter retrievals, among other things. L2 measurements are available in the 340 - 1060 nm range with a 15-min frequency with AOD mean errors of ±0.01 in the visible and near-infrared. Absolute errors are well below or about ±0.03, indicating high relative errors are due to the low Arctic background concentrations. See [9] [36] [37] for further discussion of errors.

There were 35 sites north of 59.75˚N (Figure 1) with AOD for different lengths of durations between June and October 2006 to 2020.

2.2. Data Processing for Assessment of Satellite-Retrieved Aerosol Products by Ground-Based Aerosol Observations

To assess the AOD-products at 550 nm (MODIS, MAIAC, GOES) and 532 nm (CALIOP), the AERONET L2 data were converted to these wavelengths using the same procedure as described in [12].

2.3. Data Processing for Inter-Comparison of Satellite-Retrieved Aerosol Products and Scale Analysis

To compare the spatial distribution of mean AOD at the monthly, seasonal (JJASO), and inter-annual scales, we determined CALIOP AOD at 550 nm because climate models typically provide AOD at this wavelength. We resampled the MODIS, CALIOP, and MAIAC data at 550 nm on a 0.25˚ × 0.25˚ grid using a Drop-in-Bucket method for all columnar AOD values.

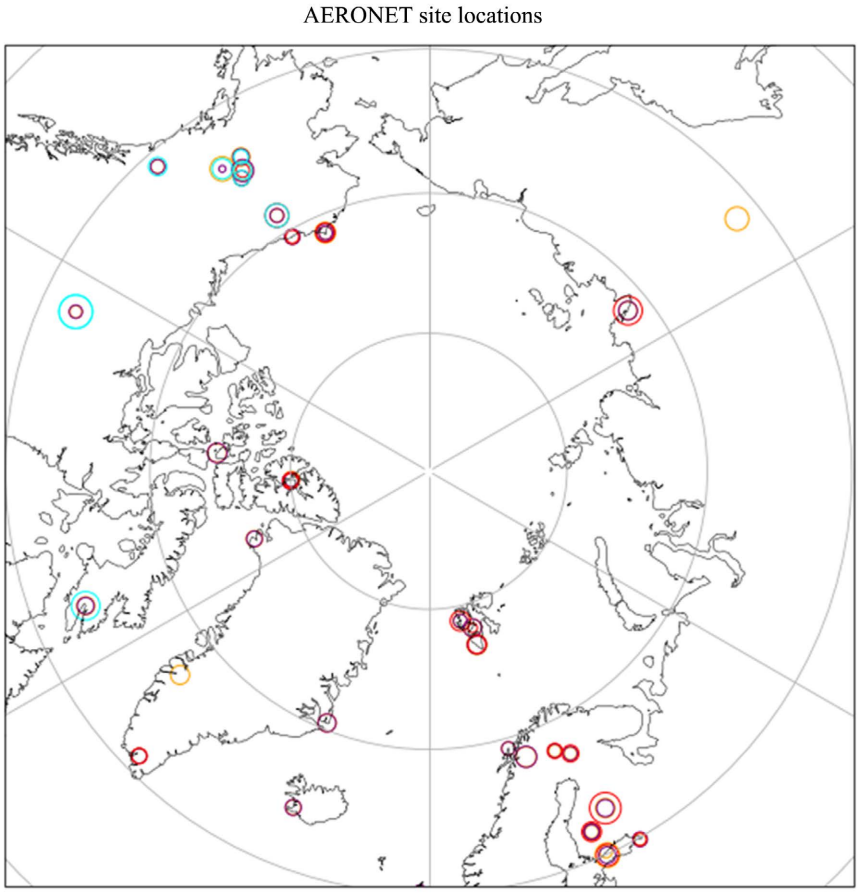

Figure 1. Location of the 35 AERONET sites considered in this study. Circles indicate the mean AERONET AOD over all available data for JJASO 2006-2020 according to the collocation of AERONET with CALIOP (red), MAIAC (purple), MODIS (orange), and GOES (cyan) observations. Smallest and largest circles indicate AOD-values of 0.038 and 0.469. Not all sites have collocation for all products.

2.4. Analysis Methods for Assessment of Accuracy, and the Role of Spatial and Temporal Scales

The comparisons of temporally high-resolved point data with spatially high-resolved data at a point in time face several well-known challenges. As aforementioned, the CALIOP, MAIAC and MODIS AOD data are grid-level means with varying spatial resolutions for each product. In contrast, ground-based data are site-specific point measurements that may yield scale-dependent representativeness errors.

Following [38], the evaluation encompassed all clear-sky AOD values regardless of their quality flags and confidence indicators. In general, both the satellite- and ground-retrieved data are subject to random errors (observational errors) and systematic errors (like the representativeness of the monitored area and timeseries, accuracy of cloud and sea ice masks, surface properties, sensor calibration, instrument sensitivity, uncertainties in the retrieval algorithms from empirical values and thresholds used in the aerosol models, etc.). Therefore, product expected errors ($EE_{product} = \pm(e_{abs} + e_{rel} \cdot \tau_{aer})$) have been derived (e.g., [5] [13]). Here e_{abs} and e_{rel} are the absolute and relative uncertainty, τ_{aer} is the AERONET AOD at the wavelength of interest, and the subscript of EE indicates the AOD-product. The combined Aqua and Terra MODIS product has an EE_{MODIS} of $\pm(0.05 + 0.15\,\tau_{aer,550})$ and $\pm(0.05 + 0.03\,\tau_{aer,550})$ over land and ocean [13], where $\tau_{aer,550}$ is the 550 nm AERONET AOD. The EE_{MAIAC} and EE_{CALIOP} are $\pm0.05 + 0.05\,\tau_{aer,550}$ [5] and $\pm0.05 + 0.4\,\tau_{aer,532}$, where $\tau_{aer,532}$ is the 532 nm AERONET AOD. Because GOES uses the MODIS instrumentation, EE_{GOES} is assumed to be that of EE_{MODIS}, $\pm(0.05 + 0.15\,\tau_{aer,550})$ [33]. For our inter-comparison, we calculated the AOD percentage within the EE envelope of $\tau_{aer} - EE_{product} < \tau_{product} < \tau_{aer} + EE_{product}$ for each site and across all 35 sites.

To compare the AOD distributions, means and higher moments (standard deviation, skewness, kurtosis) were calculated for the satellite products. In addition, the AOD medians were determined.

Low absolute errors can result in high relative errors for low AOD values. Therefore, we assessed the AOD-products using skill-score goals and criterions typically applied by the Environmental Protection Agency in model and observation data comparison [39]. Following [12] we calculated normalized mean bias (NMB), normalized mean error (NME), RMSE, and Pearson correlation skill scores. The skill-score goals and criterions were determined using collocated data pairs. Agreement of the data was tested for statistical significance at the 95% confidence using a paired, two tails student t-test following [40].

While the MODIS instrument provides information over a substantial area rectangular to the satellite overpasses, the CALIOP instrument provides only data along the nadir point. To examine the spatial scaling impact in determining collocation, cross-correlations were determined for the AOD within the 40-km radius around each pixel on the CALIOP-Aqua nadir line for the MODIS data, and along the 40-km up and down along the nadir line for the respective CALIOP

pixel. Herein the MODIS, and CALIOP pixel was assumed as an arbitrary site. The respective pixel's AOD was assumed as the "observed" AOD. To test the hypothesis that the lack of lateral information may affect the agreement of CALIOP-retrieved and ground-based AOD, we also determined the cross-correlations of MODIS AOD for each pixel on the nadir line 40-km up and down each pixel on the nadir line. Next we determined probability density functions of cross-correlations for each of the 15 JJASO, and JJASO 2006-2020 based on the obtained cross-correlations for the MODIS AOD in the 40-km radius, MODIS 40-km up and down the nadir line, and the CALIOP 40-km up and down the nadir line.

3. Results and Discussion

Typically, the satellite-borne AOD-products have no valid observations over the Greenland ice shield. From a climatological aspect in June to October 2006-2020 easterly winds dominated in the regions of most sites (cp. Figure 1 and Figure 2).

In Siberia, high emissions of particulate matter of 2.5 μm or less in diameter occurred in 2006, 2011, 2013, 2014, 2016, 2017, 2018 and 2019 due to fires; in Canada, high fire emissions occurred in 2014, 2015, 2016, 2017 and 2019; Alaska experienced strong fires in 2010 and 2015 (cf., e.g., [41]).

3.1. Temporal and Small-Scale Spatial Variability of Arctic Aerosol Optical Depth at 550 nm

AERONET AOD inter-annual variation was largest at Tiksi followed by the National Ecological Observatory Network (NEON) Barrow and OPAL sites due to strong wildfires in Siberia, Alaska and Canada, respectively.

Two sites existed close to each other at Barrow (NEON, AERONET), Helsinki

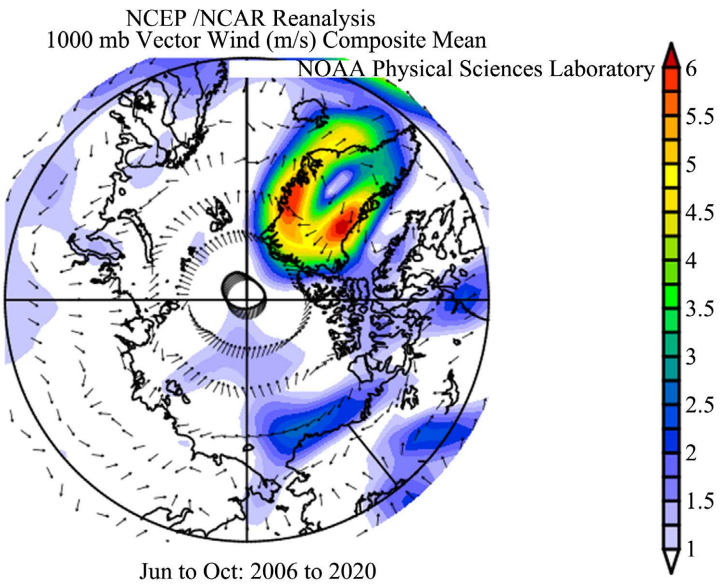

Figure 2. Composite of JJASO 2006-2020 mean wind directions and speeds over the Arctic north of 59.75˚N.

(city, lighthouse), Eureka (OPAL, PEARL), Bonanza Creek, and Hyytalia (called Atmospheric Radiation Measurement (ARM), Finish Meteorological Institute (FMI) sites hereafter). In 2014, data were only collected at the FMI Hyytalia site. In 2017 and 2019, data were collected at both Barrow sites. However, the number of MODIS collocations with concurrent data at both sites was too small for a reasonable statistic, whereas there were 22 MAIAC collocations with daily AOD at both sites. For 2020, AOD was available from two sites at Bonanza Creek.

Comparison of simultaneous observations at Helsinki revealed that the distribution of AERONET and MODIS AOD differed marginally less among the two sites than the MODIS and AERONET distributions differed at the respective site [12]. For concurrent MODIS collocations at both sites, 82.4% and 86.9% of the MODIS AOD were within the EE at Helsinki city and lighthouse. This performance exceeded those for the respective full datasets of collocation at each single site (72.9%, 82.3%) [12].

Following [12], we compared the Eureka AOD data for concurrent collocations at the PEARL and OPAL sites (**Figure 3**). For the so reduced datasets 38.1% and 57.1% of the MODIS AOD were within the expected error of the AERONET AOD at OPAL and PEARL, respectively. The comparison of PEARL and OPAL AERONET data showed 100% of these data were within the EE. MODIS AOD differed stronger among these sites than AERONET AOD (cf. **Figure 3(b)** and **Figure 3(e)**). Nevertheless, 73.9% of the OPAL MODIS AOD fell within the EE of PEARL MODIS AOD, while 75.4% of the PEARL AOD were within the EE of the OPAL AOD. These findings suggest that the algorithm struggles with the complex terrain around the Eureka sites.

The temporal evolutions of PEARL and OPAL AERONET AOD only marginally differed (cf. e.g. **Figure 3(c)**). On the contrary, MODIS AOD shows a strong temporal variation at both sites with typically lower values at PEARL. Obviously, the MODIS AOD algorithm is sensitive to blowing snow.

Together these findings suggest that the representativeness of the Earth's surface within the 40-km radius for the surface at the Arctic AERONET site strongly affects the percentage of agreement within the EE. Obviously, accuracy decreases with increasing heterogeneity within the 40-km radius of sites.

During clear-sky conditions, MODIS can provide AOD multiple times per day, whereas MAIAC provides representative daily mean AOD. Same as for MODIS, we considered MAIAC AOD only for collocations at both Eureka sites. Therefore, as a result of the lower temporal resolution, this AERONET sample differs from that used in MODIS-AERONET comparison discussed above. At OPAL and PEARL, 62% and 75.2% of the MAIAC AOD were within the EE of the AERONET AOD, respectively. Again all AERONET data were within the EE of the respective other site.

Like for MODIS C6.1, MAIAC AOD differed stronger among these sites than AERONET AOD (cf. **Figure 3(a)** and **Figure 3(d)**). Nevertheless, 77.5% of the OPAL MAIAC AOD fell within the EE of PEARL MAIAC AOD, while 78.3% of the PEARL AOD were within the EE of the OPAL MAIAC AOD. These findings

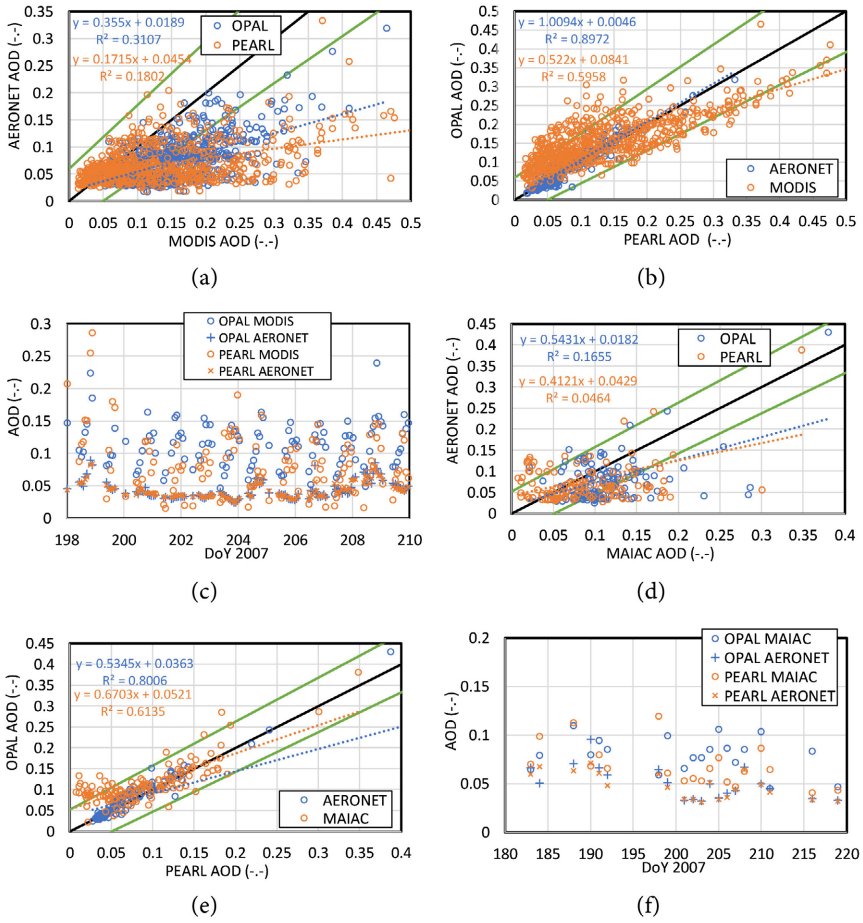

Figure 3. Comparison of retrieved AOD at 550 nm at times of concurrent collocations at the two Eureka sites for JJASO 2007-2013 and JJASO 2016. (a) MODIS retrieved AOD vs. AERONET AOD, (b) OPAL vs. PEARL retrieved AOD for MODIS. (c) Temporal evolution of AOD at OPAL and PEARL as obtained from AERONET and MODIS for an episode in 2007. (d) MAIAC retrieved AOD vs. AERONET AOD, (e) OPAL vs. PEARL retrieved AOD for MAIAC. (f) Temporal evolution of AOD at OPAL and PEARL as obtained from AERONET and MAIAC for JJASO 2007. Trendlines and their equations are in the color of data. Upper and lower EE envelop with respect to the quantity on the X-axis are green. Black is the 1:1 line. Other times and JJASO seasons show similar spread in the satellite product AOD time series and agreement in the AERONET AOD time series.

suggest that the MAIAC algorithm struggles less with the complex terrain around the Eureka sites than the MODIS algorithm.

As expected the temporal evolutions of PEARL and OPAL AERONET AOD only marginally differed (cf. e.g. **Figure 3(f)**). In contrast to the MODIS product (e.g., **Figure 3(c)**), the temporal evolution of MAIAC AOD at PEARL and OPAL agreed broadly with each other (e.g. **Figure 3(f)**). The Eureka MAIAC AOD broadly followed the temporal evolution of AERONET AOD, but with higher values. Like for MODIS AOD, MAIAC AOD was typically lower at PEARL than OPAL (**Figure 3**). Discernibly, a coarse temporal resolution improves the agreement between satellite-retrieved and AERONET AOD.

At Barrow, the AOD ground observations at both sites correlated 91%, while the MAIAC AOD values over these sites correlated 98%. However, at both sites the 21 satellite and ground retrieved AOD pairs showed no correlation. Nevertheless, 52.4% and 66.7% of the MAIAC AOD fell within the expected errors of the AOD ground observations at the Barrow AERONET and NEON sites, respectively, and 95.2% of the MAIAC NEON Barrow AOD were within the expected error of the MAIAC Barrow AOD and vice versa.

At the Bonanza Creek sites, also too few concurrent collocations existed for the MODIS product, but 21 for the MAIAC product. During wildfires MAIAC and AERONET AOD and their temporal evolution differed notably. However, after the end of the wildfire season they have the same temporal evolution at both sites. Typically, MAIAC AOD were higher than AERONET AOD at both sites, with lower AOD at the NEON Bonanza Creek site.

3.2. Assessment of Satellite-Retrieved Arctic Aerosol Optical Depth by AERONET Data

As previously highlighted, the satellite products differ in spatial and temporal resolution. To maximize the number of collocations for each product, we assessed the satellite products separately based on their individual collocations with the AERONET data.

Following the procedure for collocation described in Section 2 resulted in 88 CALIOP-AERONET pairs, 249 GOES-AERONET pairs, 3433 MAIAC-AERONET pairs, and 18559 MODIS-AERONET pairs for assessment of agreement. Due to the different spatial and temporal coverage, both MAIAC and MODIS have higher sample sizes of collocation with AERONET than CALIOP. The sample sizes of MAIAC and MODIS differ because of the different temporal resolution. Furthermore, MAIAC has more missing data than MODIS because the MAIAC retrieval over water depends on the glint angle. As previously discussed, the GOES data were only included for JJASO 2020.

The reason for the low number of CALIOP collocations as compared to the other satellite products is the following. In contrast to the passive cross-track scanning MODIS instrument, the active CALIOP instrument collects the return signal along a narrower path. Therefore, the likelihood that a site is within the 40-km radius of this path is several magnitudes smaller than that of Aqua MODIS. Furthermore, the MODIS and MAIAC AOD-products used both Aqua and Terra MODIS observations.

Due to the spatial and temporal differences of the AOD products, collocations do not exist for some products at some sites (cf. **Figure 1**). At some sites, the small number of collocations causes low percentage of AOD-values within the EE (**Table 1**).

In the following discussion, statistics include all available collocations within the June to October 2006-2020 timeframes. We refer to correlations of 0.2 - 0.39 as weak, 0.40 - 0.59 as moderate, 0.6 - 0.79 as strong, and 0.8 - 1 as very strong.

Table 1. Percentage of CALIOP, MAIAC and MODIS retrieved AOD within the expected error of the AERONET retrieved AOD considering all available collocations during June 1 to October 31 2006-2020. Percentage of GOES retrieved AOD covers June to October 2020. GOES-17 results are bold.

Site	Retrieval algorithm			
	CALIOP	GOES-16/**17**	MAIAC	MODIS C6.1
Abisko			41.7	59.3
Andenes	60		71.5	75.0
ARM Hyytiala			42.9	81.9
Oliktok Point	100		43.0	40.7
Barrow	75		41.2	60.4
Bonanza Creek		**74.2**	74.3	77.5
Helsinki			56.1	61.0
Helsinki Lighthouse			56.1	89.8
Hornsund	100		58.1	82.7
Hyytiala			58.1	63.8
Iqaluit		50	52.5	81.0
Ittoqqortoormiit			68.6	89.0
Kangerlussuaq	66.7		71.9	72.9
Kluane Lake	0	**0**	62.1	63.0
Kuopio	100		56.2	36.2
Lerwick			55.6	76.3
Longyearbyen	100		85.7	100.0
Matorova			85.7	65.0
Narsarsuaq			62.3	27.5
NEON Barrow	50	**71.4**	50.0	83.0
NEON Bonanza Creek	50		63.3	47.4
NEON Deju	100	**78.0**	66.7	55.4
NEON Healy		**60.0**	61.5	59.8
NEON Toolik Lake	100	**70.6**	63.2	84.9
Ny Ålesund			62.0	88.9
OPAL	73.7		49.4	28.2
PEARL	82.4		57.9	62.3
Peterhof			59.4	78.9
Resolute Bay	40		58.1	72.6
Reykjavik			73.3	49.1

Continued

Sodankyla			75.0	77.9
Thule	64.3		62.7	66.6
Tiksi	50		54.5	74.3
Yakutsk			0.0	41.3
Yellowknife		100		34.0
All sites	70.8	60 **58.2**	59.5	64.5

3.2.1. MODIS Collection 6.1 Arctic Aerosol Optical Depth at 550 nm

Except for Helsinki Lighthouse, Kluane Lake, and Longyearbyen, the 15-season site means were lower for AERONET AOD than MODIS. The 15-season AERONET AOD site medians exceeded those of MODIS at the Longyearbyen, NEON Barrow and NEON Bonanza Creek sites.

Based on the standard deviations (**Figure 4(c)**), skewness and kurtosis, the MODIS and AERONET obtained AOD-distributions matched best at Hornsund, Kangerlussuaq, Toolik Lake, Tiksi, and Yakutsk.

AERONET and MODIS AOD showed very strong correlation at the ARM Hyytiala, Bonanza Creek, Helsinki Lighthouse, Iqaluit, Longyearbyen, Toolik Lake, and Reykjavik sites. AERONET and MODIS AOD correlated strongly at Kangerlussuaq, Narsarsuaq, Ny Ålesund, and Peterhof (**Figure 4(c)**). At Oliktok Point, correlation was negative.

While 75.3% and 87.5% - 100% of the combined Terra and Aqua MODIS AOD data fell within the limits of EE over land and ocean, respectively for JJASO 2006-2018 [12], we found 64.5% over land for JJASO 2006-2020 (**Table 1**).

Major reasons for the comparatively lower agreement in our study are as follows. We considered two more years and 15 additional sites. Furthermore, we restricted the assessment of the aerosol products to AERONET sites only because of the marginal likelihood of collocated CALIOP-MAN as well as collocated MAIAC-MAN observations. The low likelihood is due to the low temporal and spatial resolution of CALIOP data, and due to the MAIAC product's large areas of missing data over ocean. Additionally, not many MAN observations existed north of 59.75˚N.

The soccer plot (**Figure 5(a)**) indicates acceptable agreement between MODIS and AERONET AOD for all but four sites (Narsarsuaq, OPAL, NEON Bonanza Creek, and Yellowknife) because of the high fractional mean errors at these four sites. While fractional biases fell within the limits of acceptable agreement at NEON Bonanza Creek, and Yellowknife, they reached 90.5% and 84.3% at Narsarsuaq and OPAL, respectively. At the latter sites, the mean AERONET AOD was below 0.07 (**Figure 5(b)**).

3.2.2. MAIAC Arctic Aerosol Optical Depth at 550 nm

No MAIAC-AERONET clear-sky collocations existed for Matorova and the 21 km offshore Helsinki lighthouse (cf. **Figure 1** and **Table 1**).

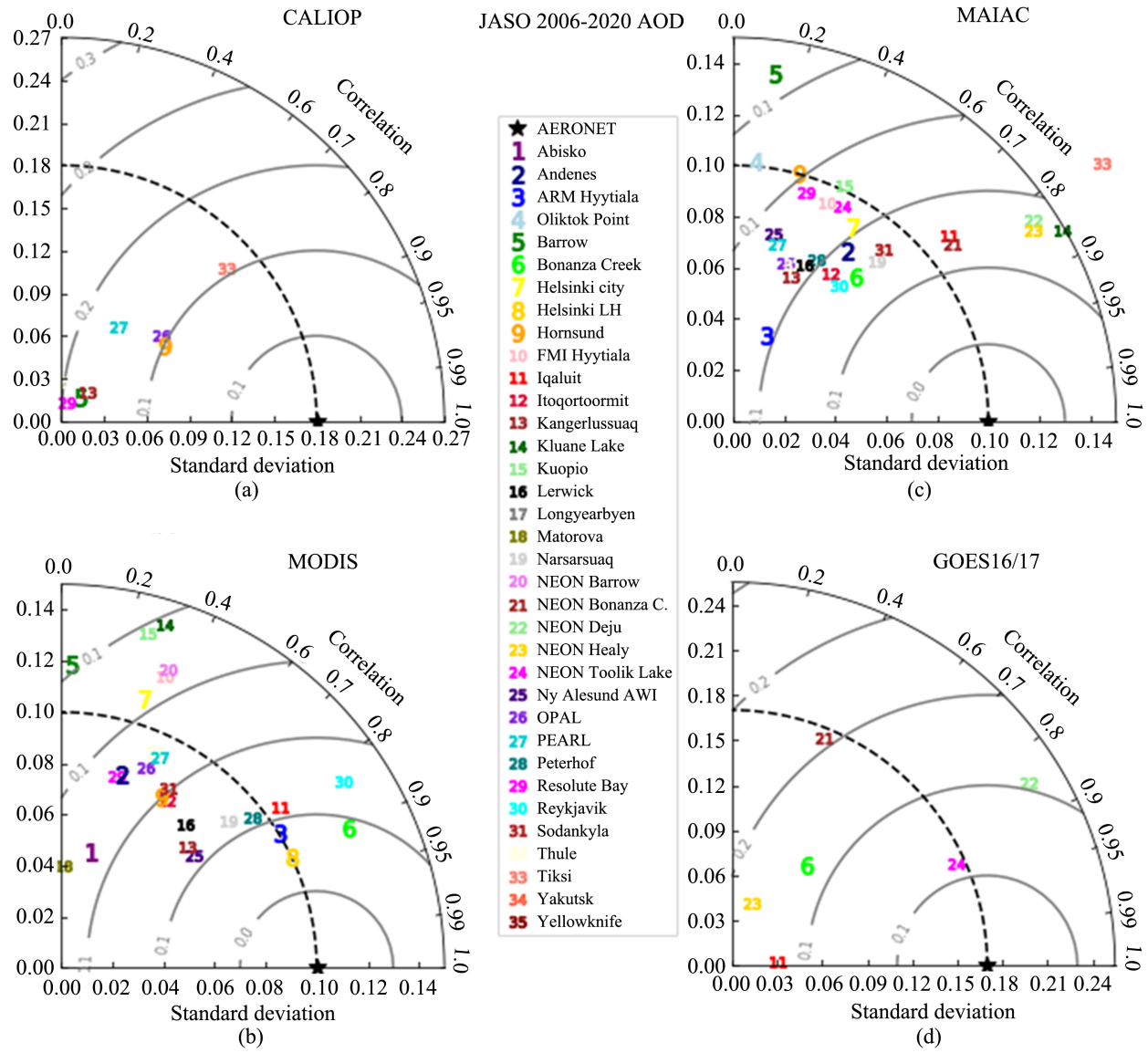

Figure 4. Taylor plot showing the June to October 2006-2020 skills for (a) CALIOP, (b) MODIS C6.1, (c) MAIAC, and (d) GOES-16/17 for all sites with collocated data. The star indicates the AERONET standard deviation over all sites with collocations and JJASO seasons. Note that the absolute value of the correlation coefficient is shown for sites with negative correlation. See text for sites and products with negative correlation.

Except for ARM Hyytiala, Longyearbyen, Toolik Lake, Petershof and Yakutsk, JJASO means of MAIAC AOD exceed those of AERONET AOD. At Kuopio, AERONET and MAIAC have the same 15-season mean. Over all sites and JJASO seasons, the bias was 0.033.

The all-season medians were higher for the MAIAC than AERONET AOD except at the ARM Hyytiala, Longyearbyen, Toolik Lake, Sodankyla and Yakutsk sites. At 12 sites, AERONET AOD seasonal standard deviations exceeded those of MAIAC (Figure 4(b)).

Overall seasons, MAIAC and AERONET AOD correlated very strongly at Kluane Lake, followed by the Healy, Deju, and Tiksi (R = 0.864, 0.845, 0.830,

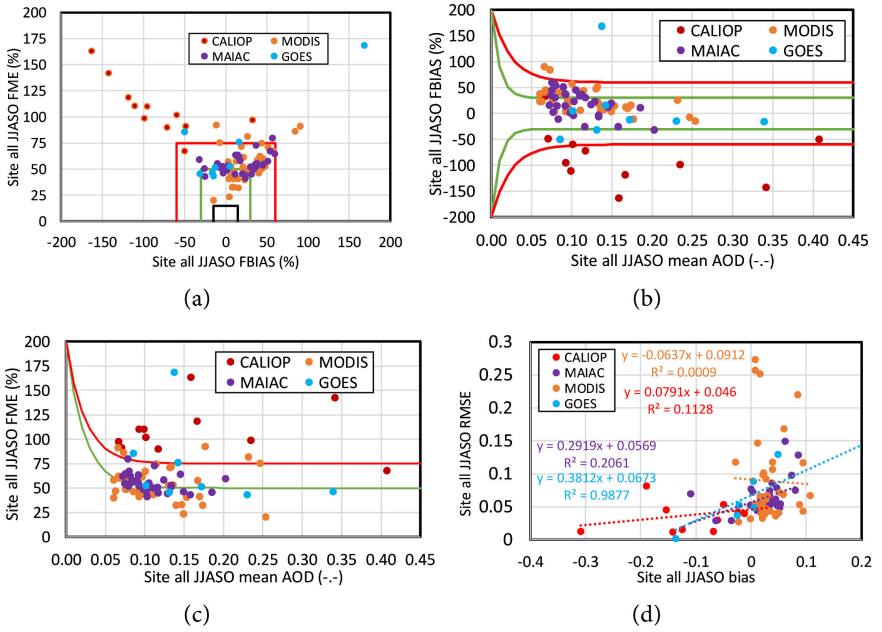

Figure 5. Skill of CALIOP, MODIS, MAIAC, and GOES retrieved AOD as compared with the AERONET retrieved AOD at 532 nm, 550 nm, 550 nm, and 550 nm, respectively, determined over all data for each site with collocation during June to October 2006 to 2020. GOES data reflect June to October 2020. (a) Soccer plot, Buggle plots of AOD-product vs. (b) fractional bias, FBIAS, (c) fractional mean error, FME, and (d) bias vs. RMSE. Green lines indicate the agreement "goals" that satellite-retrieved AOD values could achieve at their best under consideration that the AERONET-retrieved data are also subject to uncertainty due to measuremnent errors and conversion to 532 nm for the CALIOP and 550 nm for the other products. Red lines indicate the agreement "criteria" for acceptable accuracy without further evidence of adequacy. In (a), the black lines indicate the best agreement one could achieve. In (d), the bias-RMSE pair for Kluane Lake (1.4, 0.6) is not shown for readability, but included in the trendline calculation. Trendlines (dotted) and equations are in the color of the AOD-product.

0.820). Strong correlation existed for Iqaluit, NEON Bonanza Creek, and Narsarsuaq (R = 0.775, 0.757, 0.664). At Longyearbyen and Abisko, correlations were negative (R = −0.707, −0.153). The low numbers of collocation (7, 24) may be part of the reason. Considering all sites and JJASO seasons, the correlation was moderate (R = 0.489) (**Figure 4(b)**).

Over all JJASO seasons and sites, 59.6% of the MAIAC AOD fell within the limits of the EE (**Table 1**). Our results confirmed [3] that MAIAC AOD show weaker accuracy along the coasts than farther inland. Typically, a higher percentage of MAIAC AOD was within the expected error for inland sites away from lakes than for inland sites close to lakes (cp. **Figure 1** and **Table 1**).

Looking at the skewness and kurtosis suggest that the MAIAC and AERONET AOD distributions differ. Over all JJASO seasons and sites, the AERONET AOD distribution had a twice as high skewness and almost four times higher kurtosis than that of MAIAC, hinting at local sources affecting the AERONET AOD and potential temporal discrepancies affecting the comparison.

The reasons for the discrepancies between MAIAC and AERONET retrieved

AOD are as follows. MAIAC data are daily means for 1 km × 1 km. Despite using the time range of the nadir overpass, the values may include information from pixels of previous or consequent overpasses. Furthermore, the high reflectance of snow and ice reduces the number of values. However, recall that the goal of the MAIAC product was to retrieve AOD over land.

Except for Oliktok Point, MAIAC retrieved AOD fell within the goals of agreement with AERONET retrieved AOD, and outperformed the other AOD-products examined (cf. **Figure 4** and **Figure 5**).

3.2.3. CALIOP Arctic Aerosol Optical Depth at 532 nm

No collocated data existed for the two Helsinki and Hyytiala sites, Abisko, Iqaluit, Ittoqqortoormiit, Lerwick, Matarova, Peterhof, Ny Ålesund, and Reykjavík (cf. **Figure 1**). At Longyearbyen, NEON Bonanza Creek, Kluane Lake, Kuopio, and Toolik Lake only one collocation occurred each, while at NEON Barrow, Olikitk Point, and Narsarsuaq two collocation occurred.

On average over all 15 JJASO seasons, AERONET mean AOD exceeds that of CALIOP except for Oliktik Point and Narsarsuaq. Site-JJASO means of CALIOP and AERONET AOD ranged from 0.008 (Kluane Lake) to 0.217 ± 0.158 (Tiksi) and from 0.038 (Kuopio) to 0.407 ± 0.380 (Tiksi), respectively. The high values at the Tiksi site can be explained by the strong wildfires in Siberia. At all sites, CALIOP AOD showed negative bias (cf. also FBIAS in **Figure 5(b)**). Over clean Arctic Ocean regions, background AOD is typically less than 0.05 possibly explaining some of the low AOD biases.

Except for Oliktok Point, and Toolik Lake, our results confirm [21] that the CALIOP median AOD is notably smaller than that of AERONET. Except for these two sites, the median of AOD along the overpass is lower than the median of AOD within ±30 min of the overpass over the site. The higher medians for the AERONET sites may hint at local sources contributing to the AOD observed at the AERONET sites. Together these findings confirm [17] that the CALIOP retrieval underestimates weak aerosol layers when AOD is equal or less than 0.05.

Due to inter-annual variability of wildfire activity in Siberia and Canada, inter-annual variation of collocated observations at Tiksi and the Eureka sites, respectively, exceeded the 15-season JJASO means for the AERONET data, but not for the CALIOP data.

Looking at sites with 15-season JJASO means of AOD less than 0.05 reveals weak correlation except for Hornsund, Barrow, Kangerlussuaq, the Eureka sites, and Tiksi (**Figure 4(a)**). CALIOP and AERONET correlated very strongly at Hornsund ($R = 0.804$, 64.6%), strongly ($0.600 \le R < 0.800$) at Barrow, Kangerlussuaq, OPAL, Tiksi, moderate at PEARL, and determined over all sites. Correlation tended to increase with increasing 15-season JJASO mean AOD.

These results confirm [21] that in general, CALIOP and AERONET AOD show low correlation for AODs below 0.05. At the PEARL site, [21] found a large discrepancy between CALIOP and AERONET AODs. Our comparatively longer evaluation period confirms these results. Similar to MODIS, CALIOP

AOD is more likely influenced by blowing snow than the AERONET AOD in this mountainous snow-covered terrain.

At Andenes and Thule (Qaanaaq), the correlation was negative. While the sample sizes (5, 14, respectively) might play a role, both sites have in common being located in heterogeneous terrain. Consequently, depending on the dominant wind direction during the overpasses, CALIOP retrieved AOD along the flight path may fail to be representative for the local AOD at the sites. Andenes is on the northernmost point of an island surrounded by the Atlantic to all sides except the south. Thule is surrounded by mountains to three sides. When collocation occurs the Greenland ice shield is to the north and Atlantic to the south.

On average over all 15 JJASO seasons and sites, 70.8% of the CALIOP AOD were within the expected error of the AERONET data (**Table 1**). At PEARL, OPAL, and Barrow, 73.7%, 82.4%, and 75% of the CALIOP AOD were within the EE of the AERONET data.

Overall, inter-annual variation was lower for the CALIOP than AERONET AOD data. At all sites, the skewness and kurtosis of the CALIOP AOD differed notably from those found for AERONET AOD. At Oliktok Point and Resolute Bay, skewness even differed in sign. The same was true for kurtosis at Kangerlussuaq. This means the CALIOP product represents a different distribution of particles at these sites than the AERONET product.

Fractional biases were outside the criterion for acceptable agreement (**Figure 5(b)**) when judged according to Environmental Protection Agency guidance for chemistry transport model predictions [39]. Skill of the CALIOP algorithm as given by the NMB, NME, FME and FBIAS improved with distance of the site from the ocean. RMSE ranged from 0.011 (Resolute Bay) to 0.082 (Tiksi) with an overall RMSE of 0.050.

As pointed out in Section 2.4, the CALIOP product provides data only at the nadir of the CALIPSO overpass. Consequently, when determining the AOD at collocation, no information lateral to the nadir of the overpass exists. When an overpass falls within the 40-km radius of a site, there may be no CALIOP observation right over the site. It is obvious that the number of AOD-values within the 40-km radius decreases with increasing distance of the nadir line from the site.

To examine the reasons for the comparatively lower agreement statistics of the CALIOP than the other products (cf. **Figure 4** and **Figure 5**), we compared cross-correlations of the AOD up and down the nadir line that fell within the 40-km radius for both the CALIOP and MODIS products, with the cross-correlation in the 40-km radius around the site obtained for MODIS. This comparison revealed the following. Cross-correlation was typically moderate or less for AOD-values on the nadir line for both the CALIOP and MODIS products. Results slightly differed with the position of the assumed site on the nadir line. Furthermore, the spatial distributions of MODIS AOD-values determined in a 40-km radius often differed notably from those determined from MODIS AOD-values 40 km up- and down the nadir line (**Figure 6**). Cross-correlation of

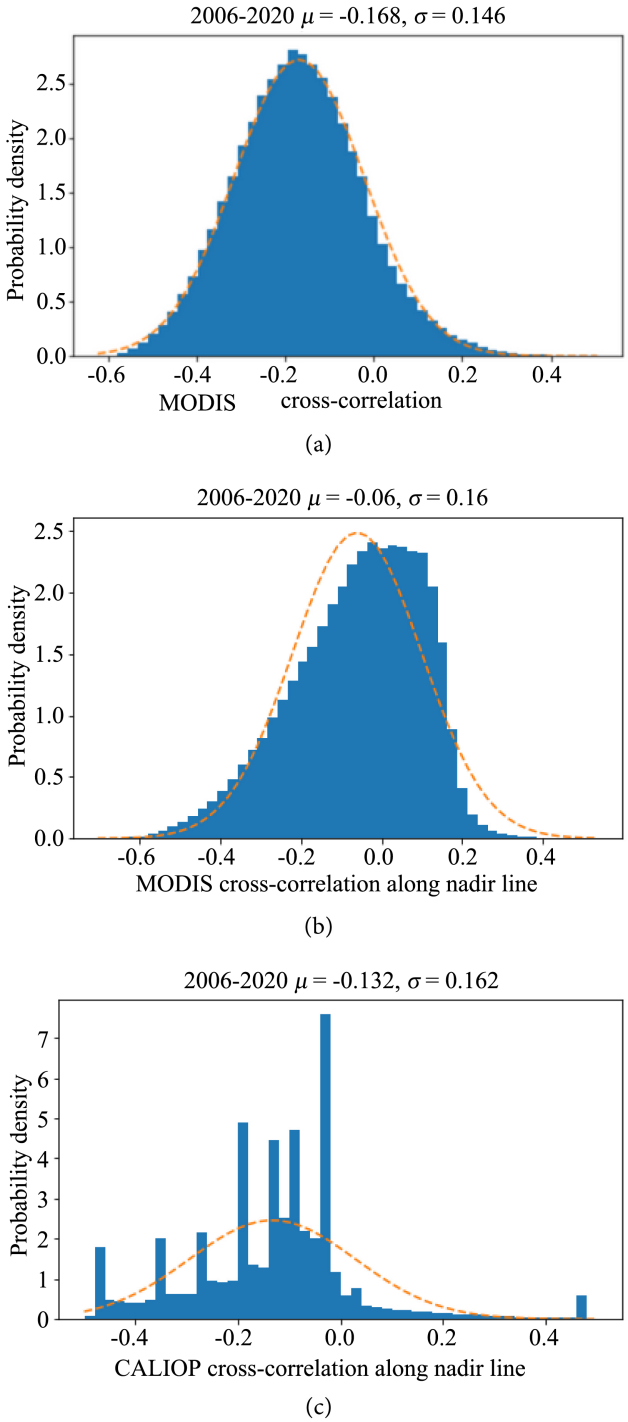

Figure 6. Probability-density distributions of cross-correlation of AOD-values for JJASO 2006-2020 (a) in a 40-km radius of each pixel on the nadir line for the MODIS C6.1 AOD-product, and 40-km up- and down the nadir line for each pixel of the (b) MODIS C6.1 AOD-product, and (c) CALIOP-product. Probability-density distributions of cross-correlations for individual years look similar to the JJASO 2006-2020 plots (therefore not shown). Note that MODIS C6.1 includes both Aqua and Terra and the increment is 3 km, while that of CALIOP is 5 km. Consequently, the sample of MODIS C6.1 is larger than that of CALIOP, and there exist more AOD-values 40 km up and down the nadir line for MODIS C6.1 than CALIOP.

MODIS AOD-values up and down the nadir line was typically lower than for MODIS AOD in the 40-km radius of the assumed sites. In general, cross-correlations were lower than the correlation between MODIS AOD and AERONET AOD or between MAIAC and AERONET AOD data.

Obviously, over all JJASO the cross-correlation of AOD-values along the nadir line strongly differs form that in a 40-km radius (cf. Figure 6). The latter results into a nearly Gaussian probability of cross-correlations. The preference for negative correlation values when only considering pixels 40-km up and down the nadir line results from the dominance of easterly winds during JJASO 2006-2020 (cp. Figure 2 and Figure 6(b) and Figure 6(c)). These results indicate that when determining collocation for the CALIOP-product, errors in collocated CALIOP AOD-values may result from missing information when the wind direction is at a large absolute angle to the overpass.

Consequently, when averaging over the data in a 40-km radius for the satellite-derived AOD and ±30 min for the AERONET AOD for collocation, CALIOP AOD might often bear errors (Figure 4(a) and Figure 5) due to the lack of information from perpendicular to the CALIPSO path (Figure 6(b)). As a result, differences between CALIOP AOD and AERONET are typically larger than for the other products.

3.2.4. GOES Arctic Aerosol Optical Depth at 550 nm

June to October means of AERONET AOD exceeded those of GOES-16 AOD at Iqaluit and Yellowknife. At the NEON Bonanza Creek, Toolik Lake, and Deju sites, Kluane Lake and Yellowknife site AERONET AOD was lower than GOES-17 AOD. Unfortunately, there was only one collocation postponing the investigations to a later date.

Except for Iqaluit, Healy and Deju AERONET AOD standard deviation was lower than the GOES AOD standard deviation (Figure 4(d)).

Bias between GOES-17 and AERONET AOD values was lowest at Deju and highest at Kluane Lake (1.445) where wildfire occurred nearby. Obviously, smoke existed in the 40-km radius of the site, but less or none right overhead the site. This statement is supported by the much lower median of the AERONET AOD (0.053) than GOES-17 AOD (1.549), the 3.4 times higher standard deviation of the GOES-17 AOD than AERONET AOD (0.174), and the notable differences between the GOES-17 and AERONET AOD distributions in both skewness and kurtosis. Furthermore, GOES-17 and AERONET AOD data showed no correlation ($R = -0.074$) and none of the former fell within the expected error of the latter (Table 1).

Correlation between GOES and AERONET AOD was very strong at Iqaluit ($R = 0.994$), Toolik Lake ($R = 0.911$) and Deju ($R = 0.851$), and moderate at Bonanza Creek (Figure 4(d)). Despite the high correlation at Iqaluit, only 50% of the GOES-16 data fell within the EE of the AERONET data (Table 1). RMSE ranged from 0.002 (Iqaluit) to 0.615 (Kluane Lake).

3.3. Inter-Comparison of the Spatial Distribution of MODIS, MAIAC, and CALIOP Arctic Aerosol Optical Depth at 550 nm

Resampling of the MODIS C6.1, MAIAC, and CALIOP AOD at 550 nm onto the same 0.25˚ × 0.25˚ grid revealed the following. In general, MODIS, MAIAC and CALIOP AOD over water are below 0.1, 0.065 and 0.05, respectively. On average over all JJASO seasons, MODIS and CALIOP provided the highest and lowest seasonal means of AOD, respectively (Figure 7).

All three products featured increased AOD over Siberia, Canada and Alaska—although comparatively lower for Canada and Alaska (Figure 7). AOD was low over ocean and data was scarce over the Greenland ice shield. Also, all retrievals seem to have difficulties in the detection of very low AOD over sea ice which leads to missing data.

Interestingly, the MODIS C6.1 AOD-product captures the smoke and particles emitted from ships traveling the Yenisei River. It also shows increased AOD over heavily traveled stretches of the Lena River (Figure 7(b)).

Obviously, the coarser resolution of the CALIOP compared to MAIAC or MODIS leads to some of the differences in the resampled 0.25˚ × 0.25˚ data (Figure 7). The likelihood for mixed scenes with respect to AOD increases with increasing area, and hence is largest for the CALIOP.

Another aspect leading to differences results from the representativeness of the resampled AOD-product for a quarter degree grid-cell. While MAIAC and MODIS actually can cover an entire grid-cell, the coarse resolution of the CALIOP product includes AOD information from outside the grid-cell into which it is resampled.

Differences between resampled seasonal distributions of CALIOP and MAIAC as well as CALIOP and MODIS AOD increase with decreasing latitude (Figure 7). This result is due under-sampling of the meridional direction in case of the CALIOP product. Because the CALIOP product delivers a 5-km wide line of AOD, the number of 0.25˚ × 0.25˚ grid cells with CALIOP AOD data decreases with decreasing latitude. Therefore, the number of AOD values from which a resampled grid-cell AOD-value is calculated, decreases as well. Furthermore, the small path means a lower temporal coverage over JJASO as compared to the MODIS instrument.

The cross-track scanning mode of the MODIS instrument namely permits application of the retrieval algorithms for a large spatial area rectangular to the flight path. Consequently, despite flying on same orbits, MODIS samples a larger area in meridional direction than CALIOP. This also means that 1) the MAIAC and MODIS retrievals get input data for every grid-cell at least once a day; and 2) the MODIS instrument can capture wildfire smoke and aerosol fields traveling over the high Arctic (Figure 7(b)).

Some differences are related to temporal aspects. CALIOP provides data at day and night, while the MODIS instrument relies on spectral reflectance, and hence depends on daylight. Consequently, the MODIS instrument provides less

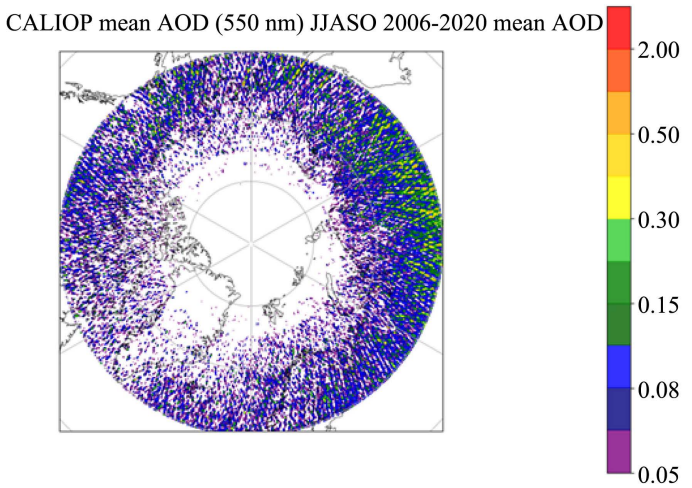

(a)

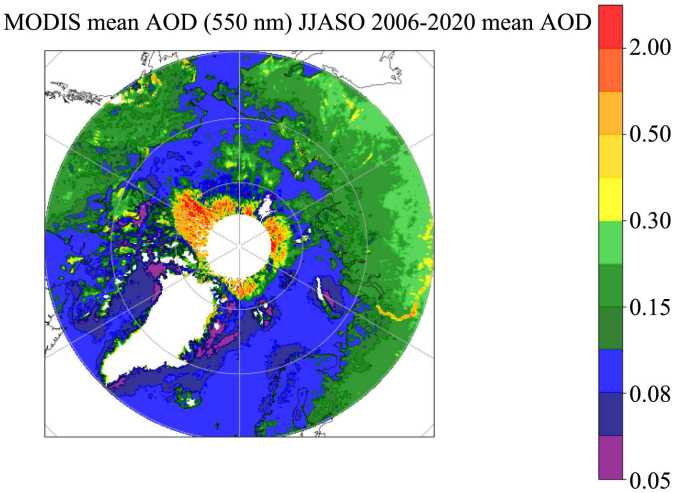

(b)

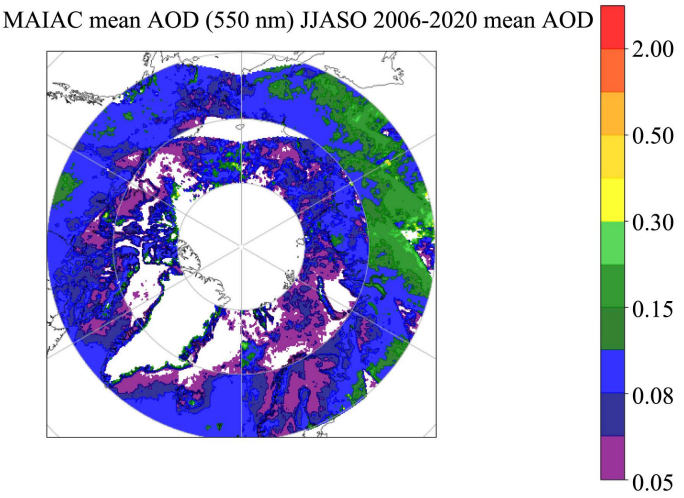

(c)

Figure 7. 2006-2020 June to October mean spatial distribution of AOD as resampled on a 0.25˚ × 0.25˚ grid for (a) CALIOP, (b) MODIS, (c) MAIAC. White areas indicate no and missing data.

data once dark nights come back than during the white nights. Because on the same day the duration of the dark night is different in the southern and northern Arctic, the amount of input data to the MAIAC and MODIS retrievals, not only changes with the sampling day in the JJASO-season, but also from north to south. However, this change differs from that discussed for the CALIOP product. A lower temporal resolution means that short events like long-distance transport over the Arctic Ocean or fast-extinguished wildfires may remain undetected. This explains the lower CALIOP AOD over Siberia as compared to the MODIS AOD (**Figure 7(a)** and **Figure 7(b)**).

Some differences between the resampled AOD distributions of the three AOD-products are due to differences in the retrievals. The MODIS retrieval obviously can capture the aforementioned smoke and aerosol transport over sea-ice (**Figure 7(b)**) in contrast to the CALIOP and MAIAC retrievals (**Figure 7(a)** and **Figure 7(c)**). The restrictions on the view angle and glint are reasons in case of the MAIAC product, while the low spatial and temporal resolution is the main cause in case of the CALIOP product.

A main reason for the low 2006-2020 JJASO mean AOD of the CALIOP product results from detected AOD below the CALIOP lower measurement limit. These detections are recorded as zero. As a result, these recordings can lead to low AOD means when resampled and averaged over time.

Another factor contributing to differences is the fact that CALIOP AOD was converted to 550 nm for comparison of the resampled distribution.

3.4. Comparison of Temporal Evolutions of Resampled MODIS, MAIAC, and CALIOP Arctic Aerosol Optical Depth at 550 nm

All three products show the same JJASO mean temporal evolution (**Figure 8(a)**). The MODIS product provides the highest AOD and changes, followed by MAIAC, and CALIOP. As expected Arctic-wide JJASO means of AOD exceeded those over oceans. The timeseries over ocean showed the same general behavior as those over the entire Arctic. This means that aerosols from wildfires govern the AOD also over the ocean due to atmospheric transport.

For both CALIOP and MAIAC marginal differences existed between the temporal evolutions of JJASO standard deviations over the ocean and entire Arctic (**Figure 8(b)**). On the contrary, timeseries of JJASO AOD standard deviations differed notably for the MODIS product.

4. Summary and Conclusions

We assessed the accuracy of CALIOP, MAIAC, MODIS, and GOES Artic AOD-products by means of 35 AERONET AOD sites north of 59.75˚N (**Figure 1**). Next we compared the spatial distribution and temporal evolution of AOD as obtained from the CALIOP, MAIAC, and MODIS products. The focus was on general agreement, scale impacts, and whether the three products can be used to detect long-term changes in AOD amount and distribution.

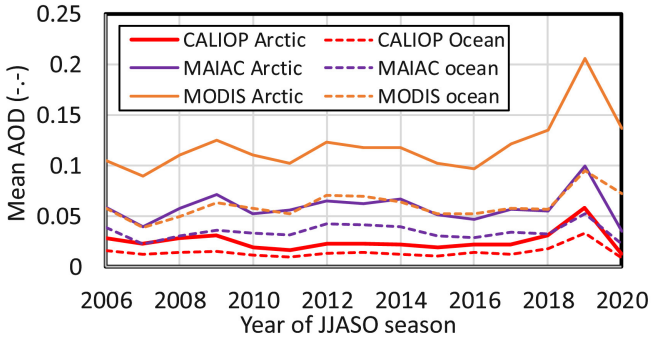

(a)

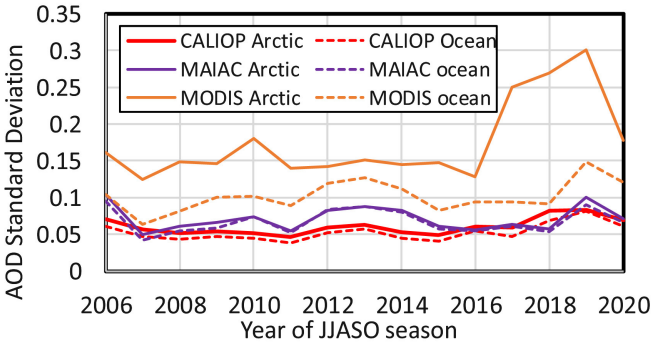

(b)

Figure 8. Time series of 2006-2020 CALIOP, MODIS, and MAIAC JJASO (a) Arctic and ocean-wide mean AOD, and (b) standard deviation. The 2020 GOES all sites JJASO mean AOD and standard deviation were 0.146 ± 0.637.

Comparison of AOD-values of the close together Eureka sites (**Figure 3**), and the two sites each in Barrow, Bonanza Creek, and Helsinki revealed that the spread between the AERONET AOD at close-by sites is smaller than that between the AERONET and satellite-derived AOD. Obviously, even within a 40-km radius and ±30 min notable differences in the AOD may occur in heterogeneous terrain. Terrain features may prohibit nearby local emissions to reach the site even when they occur within the timeslot of the overpass and in the 40-km radius of the site.

According to the results of our study, CALIOP AOD differed the strongest from the AERONET AOD (cf. **Figure 4** and **Figure 5**). Analysis of AOD cross-correlation in the 40-km radius around each pixel on the nadir line and cross-correlation of MODIS AOD 40 km up and down of the respective pixel on the nadir line (**Figure 6**) suggested that CALIOP AOD calculated for collocation often fails to be representative for the AOD at a site due to its lack of zonal information. Unfortunately, from a climatological point of view, easterly winds dominate in the Arctic [42], and dominated over the 2006 to 2020 JJASO seasons (**Figure 2**). Hence, the CALIOP AOD up and down the nadir line that fell within the 40-km radius, often failed to be representative for the AOD at a site during the ±30 min of the overpass, when the wind blew at an angle to the flight track. As a result, CALIOP AOD had lower accuracy as compared to MODIS and

MAIAC (cf. Figure 4 and Figure 5).

Comparing the sites mean AOD over all JJASO seasons reveals that MAIAC and AERONET means broadly follow a 1:1 line. MAIAC also showed the overall best agreement with the AERONET AOD (cf. Figure 4 and Figure 5). The CALIOP algorithm yields lower mean AOD at the sites than AERONET and MAIAC. The CALIOP algorithm notably underestimates the all JJASO seasons mean at sites where the means exceed 0.1. Based on these findings, one has to conclude that under clean air conditions, CALIOP cannot detect optically thin aerosol layers.

The means of the AOD-products differed notably in magnitude with CALIOP providing the lowest JJASO means and MODIS the highest. Nevertheless, on a JJASO temporal scale, CALIOP, MAIAC, and MODIS time series of Arctic-wide mean AOD broadly agree with respect to indicating JJASO seasons of low or elevated AOD (Figure 8(a)). Consequently, these AOD-products can be used to observe changes in AOD when comparing JJASO AOD means of the same product. Because of the differences among the products, it is best to assess changes in AOD as relative changes than absolute values. While the differences in temporal resolution, sample habit, sample size and scaling of the AOD-products constrain comparison analysis at the quantitative level, they permit qualitative discussion of temporal and spatial changes in AOD. Consequently, satellite-derived AOD-products can serve for qualitative assessment of chemistry transport and Earth System Models' simulated AOD changes and distributions over the Arctic for temporal and spatial scales that are much longer and larger, respectively, than those of the AOD-products. Such qualitative assessment can be valuable for gaining trust in simulated Arctic transport patterns.

Acknowledgements

We thank the AERONET, MODIS, MAIAC, and CALIOP PIs, Co-Is, and staff for establishing and maintaining the sites, algorithms, and measurements used in this investigation. We appreciate the assistance of Tyler Summers in downloading the MODIS data, and the anonymous reviewers' fruitful comments and helpful discussion. This research was funded by NASA grant 80NSSC19K0981. Mariel Friberg's research was supported by an appointment to the NASA Postdoctoral Program at the NASA Goddard Space Flight Center, administered by Universities Space Research Association under contract with NASA.

Conflicts of Interest

The authors declare no conflicts of interest regarding the publication of this paper.

References

[1] Winker, D.M., Vaughan, M.A., Omar, A., Hu, Y., Powell, K.A., Liu, Z., Hunt, W.H. and Young, S.A. (2009) Overview of the CALIPSO Mission and CALIOP Data Processing Algorithms. *Journal of Atmospheric and Oceanic Technology*, **26**, 2310-

2323. https://doi.org/10.1175/2009JTECHA1281.1

[2] NASA MODIS Adaptive Processing System, Goddard Space Flight Center (2017) MODIS Atmosphere L2 Aerosol Product.

[3] Lyapustin, A., Wang, Y., Korkin, S. and Huang, D. (2018) MODIS Collection 6 MAIAC Algorithm. *Atmospheric Measurement Techniques*, **11**, 5741-5765. https://doi.org/10.5194/amt-11-5741-2018

[4] Liu, B., Ma, Y., Gong, W., Zhang, M., Wang, W. and Shi, Y. (2018) Comparison of AOD from CALIPSO, MODIS, and Sun Photometer under Different Conditions over Central China. *Scientific Reports*, **8**, Article No. 10066. https://doi.org/10.1038/s41598-018-28417-7

[5] Wei, X., Chang, N.-B., Bai, K. and Gao, W. (2020) Satellite Remote Sensing of Aerosol Optical Depth: Advances, Challenges, and Perspectives. *Critical Reviews in Environmental Science and Technology*, **50**, 1640-1725. https://doi.org/10.1080/10643389.2019.1665944

[6] Liu, C., Shen, X. and Gao, W. (2018) Intercomparison of CALIOP, MODIS, and AERONET Aerosol Optical Depth over China During the Past Decade. *International Journal of Remote Sensing*, **39**, 7251-7275. https://doi.org/10.1080/01431161.2018.1466070

[7] Kim, M.-H., Kim, S., Yoon, S.-C. and Omar, A. (2013) Comparison of Aerosol Optical Depth between CALIOP and MODIS Aqua for CALIOP Aerosol Subtypes over the Ocean. *Journal of Geophysical Research*: *Atmospheres*, **118**, 13241-13252. https://doi.org/10.1002/2013JD019527

[8] de Oliveira, A.M., Souza, C.T., de Oliveira, N.P.M., Melo, A.K.S., Lopes, F.J.S., Landulfo, E., Elbern, H. and Hoelzemann, J.J. (2019) Analysis of Atmospheric Aerosol Optical Properties in the Northeast Brazilian Atmosphere with Remote Sensing Data from MODIS and CALIOP/CALIPSO Satellites, AERONET Photometers and a Ground-Based Lidar. *Atmosphere*, **10**, Article No. 594. https://www.mdpi.com/2073-4433/10/10/594 https://doi.org/10.3390/atmos10100594

[9] Kaskaoutis, D.G., Kharol, S.K., Sinha, P.R., Singh, R.P., Badarinath, K.V.S., Mehdi, W. and Sharma, M. (2011) Contrasting Aerosol Trends over South Asia during the Last Decade Based on MODIS Observations. *Atmospheric Measurement Techniques Discussions*, **4**, 5275-5323. https://doi.org/10.5194/amtd-4-5275-2011

[10] Campbell, J.R., Ge, C., Wang, J., Welton, E.J., Bucholtz, A., Hyer, E.J., Reid, E.A., Chew, B.N., Liew, S.-C., Salinas, S.V., Lolli, S., Kaku, K.C., Lynch, P., Mahmud, M., Mohamad, M. and Holben, B.N. (2016) Applying Advanced Ground-Based Remote Sensing in the Southeast Asian Maritime Continent to Characterize Regional Proficiencies in Smoke Transport Modeling. *Journal of Applied Meteorology and Climatology*, **55**, 3-22. https://doi.org/10.1175/JAMC-D-15-0083.1

[11] Bright, J.M. and Gueymard, C.A. (2019) Climate-Specific and Global Validation of MODIS Aqua and Terra Aerosol Optical Depth at 452 AERONET Stations. *Solar Energy*, **183**, 594-605. https://doi.org/10.1016/j.solener.2019.03.043

[12] Mölders, N. and Friberg, M. (2020) Using MAN and Coastal AERONET Measurements to Assess the Suitability of MODIS C6.1 Aerosol Optical Depth for Monitoring Changes from Increased Arctic Shipping. *Open Journal of Air Pollution*, **9**, 77-104. https://doi.org/10.4236/ojap.2020.94006

[13] Remer, L.A., Mattoo, S., Levy, R.C. and Munchak, L.A. (2013) MODIS 3 Km Aerosol Product: Algorithm and Global Perspective. *Atmospheric Measurement Techniques*, **6**, 1829-1844. https://doi.org/10.5194/amt-6-1829-2013

[14] Martins, V.S., Lyapustin, A., de Carvalho, L.A.S., Barbosa, C.C.F. and Novo, E.M.L.M. (2017) Validation of High-Resolution MAIAC Aerosol Product over South America: MAIAC/AERONET Aerosols in South America. *Journal of Geophysical Research*: *Atmospheres*, **122**, 7537-7559. https://doi.org/10.1002/2016JD026301

[15] Jethva, H., Torres, O. and Yoshida, Y. (2019) Accuracy Assessment of MODIS Land Aerosol Optical Thickness Algorithms Using AERONET Measurements over North America. *Atmospheric Measurement Techniques*, **12**, 4291-4307. https://doi.org/10.5194/amt-12-4291-2019

[16] Chernokulsky, A. and Mokhov, I.I. (2012) Climatology of Total Cloudiness in the Arctic: An Intercomparison of Observations and Reanalyses. *Advances in Meteorology*, **2012**, Article ID: 542093. https://doi.org/10.1155/2012/542093

[17] Winker, D.M., Tackett, J.L., Getzewich, B.J., Liu, Z., Vaughan, M.A. and Rogers, R.R. (2013) The Global 3-D Distribution of Tropospheric Aerosols as Characterized by CALIOP. *Atmospheric Measurement Techniques*, **13**, 3345-3361. https://doi.org/10.5194/acp-13-3345-2013

[18] Zhang, Z., Zhang, M., Bilal, M., Su, B., Zhang, C. and Guo, L. (2020) Comparison of MODIS- and CALIPSO-Derived Temporal Aerosol Optical Depth over Yellow River Basin (China) from 2007 to 2015. *Earth Systems and Environment*, **4**, 535-550. https://doi.org/10.1007/s41748-020-00181-7

[19] Schutgens, N., Sayer, A.M., Heckel, A., Hsu, C., Jethva, H., de Leeuw, G., Leonard, P.J.T., Levy, R.C., Lipponen, A., Lyapustin, A., North, P., Popp, T., Poulsen, C., Sawyer, V., Sogacheva, L., Thomas, G., Torres, O., Wang, Y., Kinne, S., Schulz, M. and Stier, P. (2020) An Aerocom-Aerosat Study: Intercomparison of Satellite AOD Datasets for Aerosol Model Evaluation. *Atmospheric Chemistry and Physics*, **20**, 12431-12457. https://doi.org/10.5194/acp-20-12431-2020

[20] Taylor, G.I. (1938) The Spectrum of Turbulence. *Proceedings of the Royal Society A*: *Mathematical and Physical Sciences*, **164**, 476-490. https://doi.org/10.1098/rspa.1938.0032

[21] Omar, A.H., Winker, D.M., Tackett, J.L., Giles, D.M., Kar, J., Liu, Z., Vaughan, M.A., Powell, K.A. and Trepte, C.R. (2013) CALIOP and AERONET Aerosol Optical Depth Comparisons: One Size Fits None. *Journal of Geophysical Research*: *Atmospheres*, **118**, 4748-4766. https://doi.org/10.1002/jgrd.50330

[22] Sayer, A.M., Munchak, L.A., Hsu, N.C., Levy, R.C., Bettenhausen, C. and Jeong, M.-J. (2014) MODIS Collection 6 Aerosol Products: Comparison between Aqua's E-Deep Blue, Dark Target, and "Merged" Data Sets, and Usage Recommendations. *Journal of Geophysical Research*: *Atmospheres*, **119**, 13,965-913,989. https://doi.org/10.1002/2014JD022453

[23] Sayer, A.M., Hsu, N.C., Bettenhausen, C., Jeong, M.-J. and Meister, G. (2015) Effect of MODIS Terra Radiometric Calibration Improvements on Collection 6 Deep Blue Aerosol Products: Validation and Terra/Aqua Consistency. *Journal of Geophysical Research*: *Atmospheres*, **120**, 12,157-12,174. https://doi.org/10.1002/2015JD023878

[24] Ichoku, C., Chu, D.A., Mattoo, S., Kaufman, Y.J., Remer, L.A., Tanré, D., Slutsker, I. and Holben, B.N. (2002) A Spatio-Temporal Approach for Global Validation and Analysis of MODIS Aerosol Products. *Geophysical Research Letters*, **29**, MOD1-1-MOD1-4. https://doi.org/10.1029/2001GL013206

[25] Superczynski, S.D., Kondragunta, S. and Lyapustin, A.I. (2017) Evaluation of the Multi-Angle Implementation of Atmospheric Correction (MAIAC) Aerosol Algorithm through Intercomparison with VIIRS Aerosol Products and AERONET. *Journal of Geophysical Research*: *Atmospheres*, **122**, 3005-3022. https://doi.org/10.1002/2016JD025720

[26] Hunt, W.H., Winker, D.M., Vaughan, M.A., Powell, K.A., Lucker, P.L. and Weimer, C. (2009) *CALIPSO* Lidar Description and Performance Assessment. *Journal of Atmospheric and Oceanic Technology*, **26**, 1214-1228. https://doi.org/10.1175/2009JTECHA1223.1

[27] Hu, Y.M., Vaughan, M., Liu, Z., Lin, B., Yang, P., Flittner, D., Hunt, B., Kuehn, R., Huang, J., Wu, D., Rodier, S., Powell, K., Trepte, C. and Winker, D. (2007) The Depolarization-Attenuated Backscatter Relation: CALIPSO Lidar Measurements vs. Theory. *Optics Express*, **15**, 5327-5332. https://doi.org/10.1364/OE.15.005327

[28] Kim, M.H., Omar, A.H., Tackett, J.L., Vaughan, M.A., Winker, D.M., Trepte, C.R., Hu, Y., Liu, Z., Poole, L.R., Pitts, M.C., Kar, J. and Magill, B.E. (2018) The CALIPSO Version 4 Automated Aerosol Classification and Lidar Ratio Selection Algorithm. *Atmospheric Measurement Techniques*, **11**, 6107-6135. https://doi.org/10.5194/amt-11-6107-2018

[29] NASA (National Aeronautics and Space Administration) (2022) CALIPSO Data User's Guide. http://www-calipso.larc.nasa.gov/resources/calipso_users_guide/

[30] Schmit, T.J., Gunshor, M.M., Menzel, W.P., Gurka, J.J., Li, J. and Bachmeier, A.S. (2005) Introducing the Next-Generation Advanced Baseline Imager on GOES-R. *Bulletin of the American Meteorological Society*, **86**, 1079-1096. https://doi.org/10.1175/BAMS-86-8-1079

[31] Schmit, T.J.G., P., Gunshor, M.M., Daniels, J., Goodman, S.J. and Lebair, W.J. (2017) A Closer Look at the ABI on the GOES-R Series. *Bulletin of the American Meteorological Society*, **98**, 681-698. https://doi.org/10.1175/BAMS-D-15-00230.1

[32] Harris-Corporation (2019) GOES-R Series Product Definition and User's Guide (PUG). https://www.goes-r.gov/products/docs/PUG-L2+-vol5.pdf

[33] Laszlo, I. and Daniels, J. (2021) GOES-17 ABI L2 + Aerosol Optical Depth (AOD) Release Provisional Data Quality. https://www.star.nesdis.noaa.gov/atmospheric-composition-training/documents/GOES-17_ABI_L2_AOD_Provisional_ReadMe_v3.pdf

[34] Aerosol Product Application Team of the AWG Aerosols/Air Quality/Atmospheric Chemistry Team (2012) GOES-R Advanced Baseline Imager (ABI) Algorithm Theoretical Basis Document for Suspended Matter/Aerosol Optical Depth and Aerosol Size Parameter. https://www.star.nesdis.noaa.gov/goesr/docs/ATBD/AOD.pdf

[35] Holben, B.N., Tanré, D., Smirnov, A., Eck, T.F., Slutsker, I., Abuhassan, N., Newcomb, W.W., Schafer, J.S., Chatenet, B., Lavenu, F., Kaufman, Y.J., Castle, J.V., Setzer, A., Markham, B., Clark, D., Frouin, R., Halthore, R., Karneli, A., O'Neill, N.T., Pietras, C., Pinker, R.T., Voss, K. and Zibordi, G. (2001) An Emerging Ground-Based Aerosol Climatology: Aerosol Optical Depth from AERONET. *Journal of Geophysical Research*: *Atmospheres*, **106**, 12067-12097. https://doi.org/10.1029/2001JD900014

[36] Kaskaoutis, D.G., Kalapureddy, M.C.R., Krishna Moorthy, K., Devara, P.C.S., Nastos, P.T., Kosmopoulos, P.G. and Kambezidis, H.D. (2010) Heterogeneity in Pre-Monsoon Aerosol Types over the Arabian Sea Deduced from Ship-Borne Measurements of Spectral AODs. *Atmospheric Chemistry and Physics*, **10**, 4893-4908. https://doi.org/10.5194/acp-10-4893-2010

[37] Kharol, S.K., Badarinath, K.V.S., Kaskaoutis, D.G., Sharma, A.R. and Gharai, B. (2011) Influence of Continental Advection on Aerosol Characteristics over Bay of Bengal (BoB) in Winter: Results from W-ICARB Cruise Experiment. *Annales Geophysics*, **29**, 1423–1438. https://doi.org/10.5194/angeo-29-1423-2011

[38] de Leeuw, G., Holzer-Popp, T., Bevan, S., Davies, W.H., Descloitres, J., Grainger,

R.G., Griesfeller, J., Heckel, A., Kinne, S., Klüser, L., Kolmonen, P., Litvinov, P., Martynenko, D., North, P., Ovigneur, B., Pascal, N., Poulsen, C., Ramon, D., Schulz, M., Siddans, R., Sogacheva, L., Tanré, D., Thomas, G.E., Virtanen, T.H., von Hoyningen Huene, W., Vountas, M. and Pinnock, S. (2015) Evaluation of Seven European Aerosol Optical Depth Retrieval Algorithms for Climate Analysis. *Remote Sensing of Environment*, **162**, 295-315. https://doi.org/10.1016/j.rse.2013.04.023

[39] EPA (2007) Guidance on the Use of Models and Other Analyses for Demonstrating Attainment of Air Quality Goals for Ozone, $PM_{2.5}$, and Regional Haze. United States Environmental Protection Agency, Washington DC, 262 p.

[40] von Storch, H. and Zwiers, F.W. (1999) Statistical Analysis in Climate Research, Cambridge University Press, Cambridge, 495 p.

[41] Randerson, J.T., van der Werf, G.R., Giglio, L., Collatz, G.J. and Kasibhatla, P.S. (2018) Global Fire Emissions Database, Version 4.1 (GFEDv4). ORNL DAAC, Oak Ridge.

[42] Mölders, N. and Kramm, G. (2014) Lectures in Meteorology. Springer, Cham, 591 p. https://doi.org/10.1007/978-3-319-02144-7